

Review

Autonomously Moving Colloidal Objects that Resemble Living Matter

Akihisa Shioi *, Takahiko Ban and Youichi Morimune

Department of Chemical Engineering & Materials Science, Doshisha University, 1-3 Tatara Miyakodani, Kyotanabe, Kyoto 610-0321, Japan; E Maile: then@mail.doshisha.aa.in (T.R.): dti0546@mail4.doshisha.aa.in (Y.M.)

E-Mails: tban@mail.doshisha.ac.jp (T.B.); dtj0546@mail4.doshisha.ac.jp (Y.M.)

* Author to whom correspondence should be addressed; E-Mail: ashioi@mail.doshisha.ac.jp.

Received: 25 *September* 2010; *in revised form:* 19 *October* 2010 / *Accepted:* 7 *November* 2010 / *Published:* 16 *November* 2010

Abstract: The design of autonomously moving objects that resemble living matter is an excellent research topic that may develop into various applications of functional motion. Autonomous motion can demonstrate numerous significant characteristics such as transduction of chemical potential into work without heat, chemosensitive motion, chemotactic and phototactic motions, and pulse-like motion with periodicities responding to the chemical environment. Sustainable motion can be realized with an open system that exchanges heat and matter across its interface. Hence the autonomously moving object has a colloidal scale with a large specific area. This article reviews several examples of systems with such characteristics that have been studied, focusing on chemical systems containing amphiphilic molecules.

Keywords: autonomous motion; colloidal objects; nonlinear dynamics; chemomechanical energy conversion

1. Introduction

Autonomous motion of colloidal objects such as droplets, vesicles, gels, and small particles gives the impression of living matter, because they can respond to changes in the surrounding environment and occasionally exhibit vectorial motion along a chemical composition gradient. The motion can resemble chemotaxis, haptotaxis, and other biological motions [1]. Their motion often begins after an induction period, as if they were able to think. The motion is driven by chemical reactions at the surface of a colloidal system. Since due to the smallness of the objects involved the specific area is very large, chemomechanical energy conversion at the surface moves them efficiently. Physicochemically, this type of energy conversion is significant in two ways. First, it requires no temperature gradient or difference for energy conversion. Chemical reactions result in a chemical potential drop that is transformed directly into motion. However, more significant is the fact that spatial gradients of thermodynamic variables such as chemical potential, temperature, and pressure are not necessary before the onset of motion but are spontaneously generated through various kinds of instabilities. In fact, these two characteristics are inherent in biological motion, which is why an autonomously moving object resembles living matter. For example, the physicochemical conditions inside a biological cell are often maintained by the active transport of ions with the help of membrane proteins [1], and the resulting difference between the internal and external chemical conditions enables many biological motions.

The induction period before the beginning of motion corresponds to the time in which macroscopic inhomogeneity develops from microscopic fluctuations through instability. For example, Marangoni instability, which is occasionally used in autonomously moving systems, expands a microscopic fluctuation of surface tension into macroscopic convection near the surface [2–4]. However, if the instability alone governed the dynamics of systems, the colloidal object could exhibit random or irregular motion with no systematic features. In most cases, nonlinear aspects of the dynamics suppress the endless growth of instability, so the system falls into a regulated dynamical mode [5]. For the Marangoni instability as an example, the Benard-Marangoni convection, which consists of a large number of hexagonal cells, is a result of such pattern formation [6]. In a hexagonal cell, internal convection occurs as long as heat transport is maintained.

The emergence of this system arises from the fact that the instability essentially causes the dynamics, and the underlying nonlinearity suppresses its endless growth so it falls into regulated motion. The resultant motion or dynamics is far beyond the conventional ones which are easily predicted by classical transport phenomena [7], in which the system approaches equilibrium at every point, making self-sustained motion almost impossible. To design continuous energy conversion in this situation, a systematic gradient of thermodynamic quantity, such as a temperature gradient, is required; this would cause heat flow (strictly speaking entropy flow). In a heat engine, the working fluid expands and contracts for the inflow and outflow of heat, respectively. These two opposite processes generate a cycle, that enables continuous energy conversion. An autonomously moving system requires no such artificial cycle. Instead, the system returns to its initial state through a cycle composed of nonlinear oscillations that arise from a combinations of instability and its nonlinear suppression [5]. The instability and nonlinear suppressions depend on the surrounding environment, e.g., the chemical composition and its spatial gradient. This is because the autonomously moving object responds to the surrounding environment.

In the first section of this review, we describe the type of dynamical features that must appear in an autonomously moving system that resembles living matter and why one sees it as an emerging chemical system. Next, we select only three kinds of autonomously moving objects from among a vast number of colloidal systems. The first is an oil/water system, whose autonomous motion is probably the most studied among many colloidal systems. Chemical reactions or ion exchange at the oil/water

interface cause oscillatory changes in the interfacial tension and/or in the contact angle on a solid substrate. These nonlinear dynamics maintain its self-sustained motion. The characteristics of motion, often called the dynamical mode, are controlled by reactive chemicals, *i.e.*, by their concentration, species, and concentration gradient. In a particular case, this type of droplet can solve a maze even though it is not intelligent. The second object is a vesicle that spontaneously moves by chemical reactions in or near the membrane. This type of study is inspired by biological studies of amoeboid and bacteria motions, which move by biological reactions catalyzed by membrane proteins. Although a vesicle may be regarded as a model cell, it is not alive and moves autonomously by simpler physicochemical processes. The last one consists of small particles. A particle often works as a catalyst that accelerates the reaction rate near the surface. Chemical reactions at or near the particle surface provide the kinetic energy of particle motion. As another type of solid particle, a piece of camphor or a camphor float is a well-known autonomously moving object. Studies of such particle locomotion are reviewed.

2. Emergent Behavior and Autonomous Motion

The emerging chemical systems discussed in this paper contain nonlinearity in their dynamics. This is essential for their self-sustained motion. In this section, we discuss the relationship between the nonlinear dynamics and their emerging nature. Although it may be a primitive description of this field, explicit descriptions are rarely seen as far as the authors know.

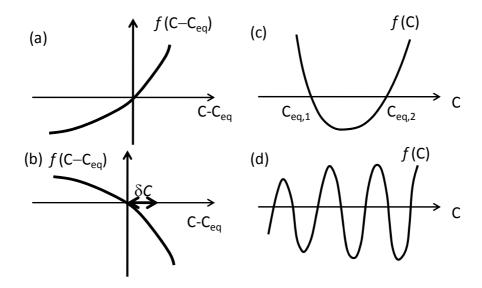
Thermodynamics states that the whole system including a treated chemical system and its environment reaches equilibrium after a sufficiently long time. For example, a difference in concentration disappears by mass transport or diffusion until the system attains equilibrium defined by a constant chemical potential. Focusing on a local system, however, it does not necessarily go to equilibrium monotonously. Consider a chemical system in which mass transport and/or chemical reactions are allowed. We denote the local concentration of a certain chemical species as *C* in that system. We consider the concentration instead of the chemical potential for simplicity. After the system reaches equilibrium, the concentration becomes C_{eq} The rate of the concentration change at that point may be expressed as a function of the difference, $C - C_{eq}$. Thus, we may express the concentration change at the point by the following expression:

$$\frac{dC(t)}{dt} = -f(C - C_{eq}), \quad f(C - C_{eq}) = 0 \text{ at } C = C_{eq}$$
(1)

The second equation demonstrates that the concentration no longer changes once it reaches the equilibrium value. Most typically the function f(C) represents the rate of mass transport or the rate of the chemical reaction. In the former case, C_{eq} represents the homogeneous concentration after diffusion. In the latter, C_{eq} stands for the concentration at chemical equilibrium. The minus sign of the right-hand side of the first equation guarantees that f(x) increases with increasing x, as explained below. The curve of f(x) under these restrictions is shown in Figure 1a. Consider a case in which the local concentration C is larger than C_{eq} . Then, $C - C_{eq}$ is positive and $f(C - C_{eq})$ is also positive. Thus, the concentration decreases because of the minus sign of Equation 1. As a result, C can become C_{eq} . When the initial concentration C is lower than C_{eq} , the concentration increases with time to reach C_{eq} .

This is a typical transport phenomenon or reaction kinetics reflecting the second law of thermodynamics. In this case, the system is stable against fluctuations in the concentration.

Figure 1. Schematic representation of f(x), which controls the dynamics of a system, for (a) a stable system, (b) an unstable system, (c) a possible transition from unstable to stable points and (d) an emerging system.



Consider another system in which f(x) decreases with increasing x. (See Figure 1b.) The concentration is homogeneous at C_{eq} over the system, and small localized fluctuations in concentration, $\delta C > 0$ occur. Then, $C - C_{eq}$ is positive, and hence the right-hand side of Equation 1 is also positive. As a result, C increases with time, which indicates infinite growth of the fluctuation δC . If $\delta C < 0$, the negative fluctuation also grows infinitely. This system looks unstable. In a real system, however, such infinite growth in concentration is never allowed because of other chemical reactions and/or the mass conservation law. Therefore, even if such a system really exists, a certain mechanism that is not considered in Equation 1 begins to work. This suppresses the infinite growth, and the concentration goes to another value at which a dynamical balance is maintained. Such a system is intuitively illustrated by Figure 1c. The concentration leaves $C_{eq,1}$ for the other value, $C_{eq,2}$. The function f(x) must be curved to include the other stationary concentration $C_{eq,2}$. In this illustration, the concentration of the chemical system seems to jump from $C_{eq,1}$ to $C_{eq,2}$ by concentration fluctuations or noise. This behavior is generated by the non–zero curvature of f(x), which we refer to as nonlinearity.

Consider a system for which f(C) is expressed by Figure 1d. Many points satisfy f(C) = 0. Among them, the concentration with positive (negative) dC(t)/dt is stable (unstable). If a small perturbation is applied to the stable state, the system maintains its state. However, if a larger perturbation is applied, the concentration leaves the initial value for the next stable one. This indicates that the concentration of the system changes discontinuously with perturbations applied by the surrounding environment. If such a chemical system really exists, we consider that it changes by responding to environmental changes. We treat this emergent behavior in this paper.

We discussed a single-parameter system in Figure 1. If the system contains two or more parameters such as C_i , where C_i represents the concentration of chemical species *i*, it can generate cyclic changes in concentrations. The dynamics of this type of chemical system is fully discussed in many references that cover oscillatory reactions such as the Belousov-Zhabotinsky reaction [8-10], and hence the details are not given in this paper. The point here is that a nonlinear system with two or more variables can exhibit cyclic changes or more complicated (chaotic) dynamics. (It should be noted that chaotic dynamics appears for a system with more than three variables.) In autonomously moving objects, oscillatory phenomena are essential for self-sustained (continuous) motion. Autonomous motion is a kind of continuous energy conversion from chemical potential into mechanical work. Unless an oscillatory cycle is contained in the system, it exhibits a monotonous change towards equilibrium. Energy conversion with this characteristic generates only transient power; the mechanical power generated by the explosion of a bomb is example of the transient energy conversion. However, this is not a self-sustained system. If a system continuously converts the form of energy, it must contain a cyclic process that returns the system to its initial state so it can enter the next cycle. Thus, oscillatory physicochemical processes are necessary in an autonomously moving system. In fact, many oscillatory physicochemical processes such as heart beat and circadian rhythms operate in our bodies, and are crucial to our biological functions.

All the characteristics for emergence discussed here require mass transport across the interface between the system and the surrounding. All chemical systems without it go to equilibrium monotonously, which means that the system cannot have the characteristics shown in Figure 1d. The emerging nature treated in this paper appears only in an open system far from equilibrium.

The three types of autonomously moving objects considered in this paper are droplets, vesicles and solid particles. Some exhibit self-sustained motion and contain cyclic physicochemical processes driving the motion. However, others are moved by transient physicochemical processes through which the system reaches equilibrium. Strictly speaking, this type of system is not an autonomously moving system. However, the study of such transient motion may lead to a breakthrough study for the design of self-sustained motion. Thus, we will also treat such systems in this paper. We will clearly specify the type of each system we discuss.

3. Autonomously Moving Droplet

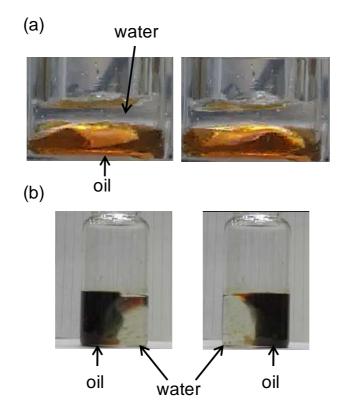
3.1. Reactive Droplet on Solid Substrate

Spontaneous droplet motions are categorized into two types. The first type uses a pretreated substrate that provides surface energy gradient. In such a system, as an example, hydrophilicity (hydrophobicity) changes gradually on a substrate, and a droplet moves so that the total interfacial energy decreases. This type of droplet motion has been studied, beginning in 1990s [11–18], and is certainly spontaneous. However, a gradient of a thermodynamic variable is required before the onset of motion. Thus, it may be categorized into the same group as a heat engine. In contrast, the second locomotion type does not require the pretreatment of a solid substrate nor, in some cases, the substrate itself. Instabilities such as Marangoni instability and/or wetting instability allow microscopic fluctuations in interfacial properties to develop into macroscopic motion. Various kinds of droplet motion appear in another immiscible liquid phase that is completely homogeneous. Chemical reactions

at or near the interface trigger instability, and hence the motion is chemically controlled. One of the most well-known examples is the oil/water system discovered by Dupeyrat and Nakache [19,20].

Dupeyrat and Nakache discovered the self-agitation of an oil/water interface that is not droplet shaped. The typical oil phase is nitrobenzene that contains iodide. Potassium iodide is saturated; the aqueous phase dissolves a cationic surfactant, *i.e.*, trimethyloctadecylammonium chloride ($C_{18}TAC$). When the lighter aqueous phase is gently poured onto the heavier oil phase, the contact line between the oil/water interface and the glass wall moves violently. In most cases, the spontaneous motion develops into wave trains [21,22], as shown in Figure 2a. The amplitude is around several mm to 1 cm. When the specific gravity of oil is close to unity, the amplitude becomes extraordinarily large. Figure 2b shows an example where the specific gravity of the oil phase is almost unity because a mixed solvent of nitrobenzene and toluene is used [23]. The oil/water interface stands up in a cylindrical container and rotates with almost constant angular velocity.

Figure 2. Spontaneous motion of oil/water system. Oil phase is nitrobenzene containing (a) 1.5 mM I₂ and (b) 50 mM I₂. KI is saturated. $C_{18}TAC$ concentration is the same as that of I₂ for each system. The right photograph is of 0.13 s (upper) and 0.46 s (lower) after the left.



Such spontaneous motion of an oil/water system containing a surfactant may be understood in terms of the Marangoni instability, which can induce vertical motion similar to that in Figure 2a. Marangoni instability is generated by local fluctuations in interfacial tension that cause the fluctuations in the curvature of the interface [6]. However, this cannot explain the motion in Figure 2b. Furthermore, the self-agitation does not appear in a container made of perfluoroethylene (PFA) [24]. The PFA container does not adsorb the surfactant, and hence the surface hydrophobicity (hydrophilicity) remains almost unchanged. These results indicate that this self-agitation is caused by a change in the surface properties

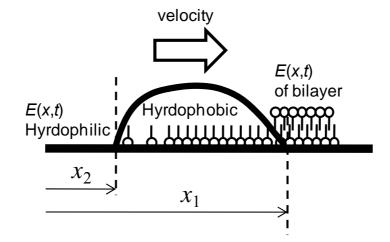
of glass. The glass surface is negatively charged for pH values larger than the isoelectric point pH ≈ 2 . Thus, the cationic head group of $C_{18}TA^+$ is adsorbed onto the glass surface [25]. The surface becomes less hydrophilic and is wetted by oil. After the oil phase wets the glass surface, polyiodide anions in the oil phase react with the adsorbed $C_{18}TA^+$ [26]. The reaction product is nonionic and oil soluble and hence is desorbed from the glass surface, which becomes hydrophilic again. As a result the glass surface is wetted by the aqueous phase, and an oscillatory cycle is thus established. Though Marangoni instability may contribute to the motion, its role is probably secondary.

When an oil droplet is placed on a glass surface immersed in the aqueous phase, the variation in the surface properties of the glass drives the droplet. (Marangoni instability may contribute to the droplet motion, but its contribution is unclear at present.) The droplet's motion can be regulated by the experimental setup. Yoshikawa *et al.* successfully controlled the dynamical mode of droplet motion [27–29], especially for the $C_{18}TAC$ /iodide system. Examples of the dynamical modes are a droplet repeating forward and backward motion, one–way motion in a closed loop standing vertically, revolution of a droplet in a glass bowl around a plumb line, and climbing glass stairs (never descending) [27–29]. All the dynamical modes can be explained by mathematical models taking into account the change in surface properties. One of the simplest models they proposed is shown in Figure 3 and is expressed as follows [29]

$$\sigma \frac{d^{2} x_{1}}{dt^{2}} = -\mu_{0} \frac{dx_{1}}{dt} - \frac{\partial E}{\partial x}\Big|_{x=x1} - \beta(r_{0})(x_{1}(t) - x_{2}(t) - r_{0})$$

$$\sigma \frac{d^{2} x_{2}}{dt^{2}} = -\mu_{0} \frac{dx_{2}}{dt} - \frac{\partial E}{\partial x}\Big|_{x=x2} - \beta(r_{0})(x_{2}(t) - x_{1}(t) + r_{0})$$
(2)

Figure 3. Motion of reactive droplet driven by surface energy gradient on a solid substrate.



Here, σ , μ_0 and r_0 denote the mass of the droplet, the viscous damping coefficient, and the characteristic size of the droplet, respectively. Also, x_1 and x_2 represent the position of the front and the rear, respectively, of the moving droplet on the *x*-axis, where one dimensional motion is considered. *E* denotes the surface energy of the glass, which is affected by the adsorption density of C₁₈TA⁺. The adsorption density depends on the ad/desorption rate and surface diffusion of C₁₈TA⁺ on glass. The adsorbed C₁₈TA⁺ is desorbed by reactions with oil-soluble anions. Thus, the adsorption density at the

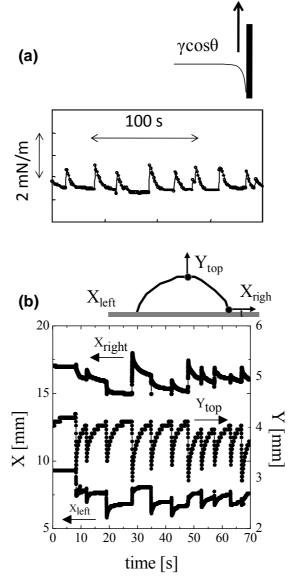
rear of the moving droplet is much less than that at the front: On the track of the moving droplet, no adsorbed $C_{18}TA^+$ remains, because the oil droplet scavenges the adsorbed $C_{18}TA^+$. Thus, the hydrophilicity of the glass surface is much higher at the rear than at the front. This difference generates the driving force expressed by the second term of the right-hand side of Equation 2. The last term of Equation 2 represents the elastic properties of a droplet with the elastic constant β (r_0). Equation 2 demonstrates that the droplet is driven by the exchange of $C_{18}TA^+$ between the bulk solutions and the glass surface so that the free energy of the whole system decreases monotonously. Focusing on the droplet itself, however, the gradient of the adsorption density is maintained by the notion itself. This is a kind of self-sustained or autocatalytic process: the motion itself generates the next step required for maintaining its dynamical state. This autocatalytic process is suppressed by viscous damping and the elastic stress of droplet deformations. This simple model can capture the essential features of droplet motion.

The above model explains droplet motion and cannot be applied to the self-agitation shown in Figure 2a. The oscillatory wetting that causes the self-agitation results from the adsorption of surfactant followed by desorption with reactive chemicals in the oil phase. This suggests that the dynamical mode can be controlled by anionic chemicals in the oil phase. Actually, using bis(2ethylhexyl)phosphate (DEHP) and phenylborate (PB) qualitatively changes the interfacial motion [30]. When DEHP is contained in oil, the contact line between the oil/water interface and the glass surface exhibits abrupt wetting by oil followed by gradual dewetting (wetting by water). Figure 4 shows the amplitude of oscillatory wetting [31], which occurs for both a vertical glass wall and a horizontal glass surface. The oscillation occurs on a restricted length of the contact line even when the contact line is sufficiently long. The restricted length is of the order of 1 mm. After the oscillation occurs, an induced wave occasionally travels along the contact line. If oil and water are set in a cylindrical glass to form a flat oil/water interface, a traveling wave with small amplitude propagates. In contrast, when an oil droplet is placed on a glass surface and immersed in the aqueous phase, a small wave travels along the periphery of the droplet, flattening. After this shape change, a reverse transition from a flattened to a bell-shaped droplet proceeds. This shape change repeats, at least, several times, as shown in Figure 4b [31].

When PB is used instead of DEHP, the oil-droplet translates on a glass surface [30]. (If a flat oil/water interface forms in a cylindrical glass container, no observable motion of the contact line is seen.) Since nothing happens in the absence of PB and DEHP, the chemical reaction between them and $C_{18}TA^+$ controls the dynamics.

The details of the control mechanism are still unclear. However, the partition coefficient of the anionic chemicals into the water phase can be considered to play a key role [30]. As shown in Figure 5, the wetting by oil requires a chemical reaction of the outer leaflet of the adsorbed layer and the anionic chemical in the water phase. Since the anionic chemical is dissolved in oil, it must move to the water phase for the reaction to occur. DEHP is more hydrophobic, and its partition coefficient to water is smaller. If the chemical desorption rate of $C_{18}TA^+$ is diffusion-limited, the overall desorption rate for a DEHP-containing system should be slower than that for a PB-containing system. Following a mathematical model discussed in the next paragraph, the instability that drives the abrupt wetting by oil occurs when the overall reaction rate is strongly diffusion-limited.

Figure 4. Oscillatory motion of contact line: (a) $\gamma \cos\theta$ for vertical glass surface and (b) oscillatory shape change between flattened and bell-shaped droplets. Oil phase contains 100 mM of DEHP, and 1.15 mM of C₁₈TAC is dissolved in the aqueous phase.



One of the most important points for elucidation of the oscillatory wetting is to understand why the abrupt wetting by oil proceeds and why it is suppressed, resulting in dewetting (wetting by water) [32]. Figure 5 illustrates the oscillatory wetting. In thermodynamic terms, $C_{18}TA^+$ molecules are adsorbed onto the glass surface as a bilayer, although the layer may have numerous defects. The overall reaction rate r_1 is determined by the reaction rate constant k and the mass transfer coefficient K. It is expressed as follows:

$$r_i = \frac{C_{A,i}}{\frac{1}{k_i} + \frac{1}{K_i}} \tag{3}$$

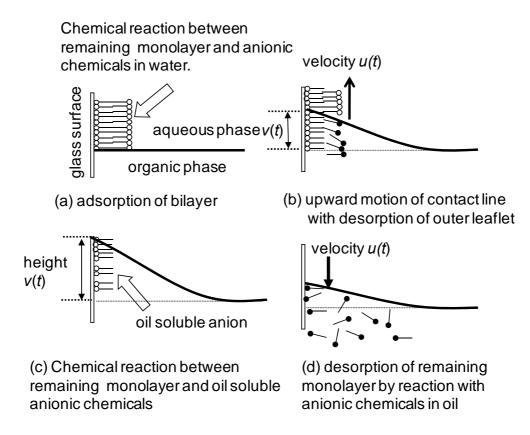
Here, C_A is the concentration of anionic chemicals. The subscript *i* is up or down, representing upward and downward motion, respectively. $C_{A,up}$ and $C_{A,down}$ are the concentrations in the water phase and in the oil phase, respectively. According to the film theory, the mass transfer coefficient *K*

increases as the convection near the contact line grows [7]. Most simply, we can assume that *K* is proportional to the speed of contact line motion |u|. Since the values of *k*, *K* and *C*_A for upward motion are different from those for downward motion, we obtain the following expression:

$$r_{up} = \frac{\kappa_{up} |u|}{1 + \frac{|u|}{k_{up}}}, \quad r_{down} = \frac{\kappa_{down} |u|}{1 + \frac{|u|}{k_{down}}}$$
(4)

Here, the subscripts up and down correspond to upward and downward motion, respectively. The proportional constant between *K* and |u| is included in κ_i and k_i . They are essentially the mass transfer coefficient and $C_{A,i}$ (κ_i) and the reaction rate constant (k_i).

Figure 5. Schematic representation of oscillatory wetting of oil/water interface at a glass surface.



Equation 4 indicates that the overall reaction rate accelerates with increasing contact line speed. Consider a weak perturbation exerted on the contact line. Even if it is very weak, it can accelerate the reaction rate. This results in a rapid change in the surface state of the glass. Thus, as the contact line speed increases, the interfacial force for a liquid phase to wet the surface strengthens, accelerating the contact line motion. In this way, the motion becomes macroscopic. However, the viscous drag force increases with increasing contact line speed. Furthermore, gravity suppresses large-amplitude motion unless the specific gravity of oil is exactly unity. These considerations are taken into account by adding $-\mu u$ for viscous drag and $-\chi v$ for the gravity effect, where v represents the amplitude, *i.e.*, the integral of u with respect to time. Therefore, we obtain:

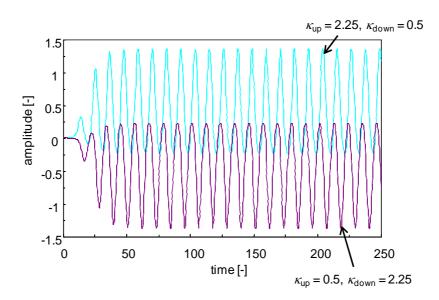
$$\frac{du}{dt} = -\mu u - \chi v + \frac{\kappa_i |u|}{1 + \frac{|u|}{k_i}} + \xi(t)$$
(5a)

$$\frac{dv}{dt} = u \tag{5b}$$

where the subscript is up for u > 0 and down for u < 0. A required perturbation is introduced as a noise term $\xi(t)$.

Figure 6 shows the calculated v(t). The sequence of pulses is obtained. The amplitude and frequency depend on the concentration of anionic chemicals $C_{A,i}$ and the specific gravity of oil χ . The dependency agrees with the trend observed experimentally [32,33].

Figure 6. Oscillation amplitude calculated by Equation 5. Both upward and downward pulses are reproduced. Parameters are $\mu = 1.0$, $\chi = 0.40$, k = 1.0, $10^{-4} < \xi(t) < 10^4$ in common. The other parameters are shown in figure. $\xi(t)$ is applied only at initial.



Equation 5 shows the oscillation of the contact line. Consider a flat oil/water interface in a cylindrical container. If the contact line oscillates at many places along the contact line, its shape becomes irregular, increasing the interfacial area. This is unfavorable from a thermodynamic point of view. Thus, the phases of the oscillations tend to be synchronized so that the interfacial area diminishes. This effect can be taken into account by introducing the second derivative of u with respect to x [34]. This yields a kind of reaction-diffusion type equation that generates traveling waves and the wave trains seen in experiments.

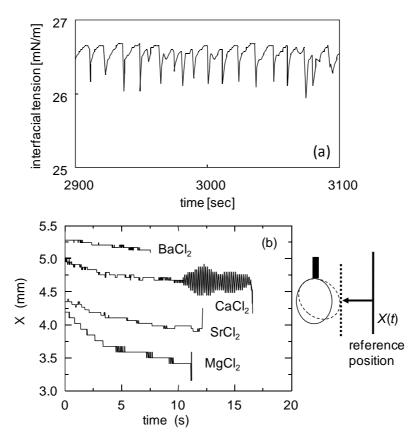
3.2. Droplet Motion without Solid Substrate

Instabilities causing macroscopic droplet motion occur in oil/water interfaces without substrates. A classical example is the kicking of a droplet by diffusion of surfactant onto the interface [35]. A sudden decrease in local interfacial tension produces a pressure gradient in the droplet, because the interfacial tension and the internal pressure are related by the Laplace equation. The pressure gradient

generates an internal flow that acts as the engine of the kicking. If the oil/water interface becomes unstable with droplet growth, the droplet exhibits various types of motions such as kicking, rotation, and pendulum motion [36]. Many variations on this type of moving droplet exist. In this paper, we treat two types of moving droplets that we can see as they emerge: ion-sensitive motion and maze-solving droplets.

An oil phase containing DEHP spontaneously exhibits Marangoni instability when Ca^{2+} is dissolved in the coexisting water phase [37,38]. However, the instability is much weaker or almost invisible when the water phase contains Ba^{2+} , Sr^{2+} or Mg^{2+} [39,40]. The instability can be observed in three types of experiments; the oscillation (or fluctuation) of interfacial tension, irregular interfacial flow in an oil/water interface and the motion of a pendant droplet. Figure 7 shows an example of tension oscillation and droplet motion.

Figure 7. Oscillation or fluctuation of interfacial tension shown as (a) the tension itself and (b) droplet motion. Oil phase contains 5 mM of DEHP; 5 M of CaCl₂ is dissolved to yield Figure 7a, and 1M of the corresponding electrolyte is dissolved for Figure 7b.

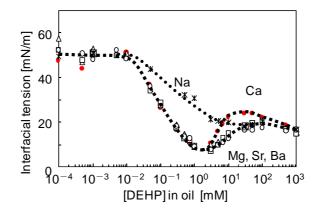


Both are closely related to Marangoni instability at the interface as discussed elsewhere [36,38]. As usual, the onset of Marangoni instability is discussed in terms of hydrodynamics. Then, the critical value of a dimensionless number such as the Marangoni number gives a criterion for onset [2–5]. This is probably applicable to the present oil/water system. However, the sensitive dependence on the ion species suggests that another type of instability may be hidden behind the hydrodynamics.

Figure 8 shows the equilibrium interfacial tension of this oil/water system [38,39]. A Ca-containing interface exhibits higher interfacial tension than others when the DEHP concentration is high. This

indicates that DEHP molecules lose their surface activity in the presence of Ca^{2+} , that is, the reaction product of Ca^{2+} and DEHP (hereafter indicated by CaDEHP) is not effective as a surfactant compared to ionized DEHP or compounds with other cations. DEHP molecules extract cations from water to oil.

Figure 8. Equilibrium interfacial tension *versus* DEHP concentration. Aqueous phase contains 1 mM of a hydroxide with divalent cations. NaOH concentration is 2 mM. Organic solvent is *n*-heptane.



Under basic conditions, the extraction proceeds mainly by electrostatic interaction between the ionized DEHP and cations. In acidic conditions, the electrostatic interaction no longer operates, and the extraction ratio decreases drastically. However, the extraction ratio of Ca^{2+} remains higher than that of other cations [39]. This indicates that some of the reaction products (CaDEHP) are oil soluble. In general, an oil-soluble compound is nonionic, and thus the surface activity of oil-soluble CaDEHP is probably less than that of ionized DEHP. This suggests that the compound CaDEHP with lower surface activity tends to be dissolved in the oil phase. Figure 9 illustrates a system with these characteristics being set under the nonequilibrium state. DEHP is adsorbed from the bulk oil to the interface and ionized. Then, the interfacial tension decreases. During adsorption, the reaction (ion exchange) between H^+ and Ca^{2+} proceeds, and the reaction product CaDEHP accumulates at the interface. If we assume that the desorption rate of CaDEHP to the bulk oil is relatively slow because of its aggregation in the interface, a large amount of CaDEHP molecules accumulates transiently. This increases the interfacial tension. Since desorption occurs in the form of aggregate desorption, numerous small holes where CaDEHP aggregates are absent are generated in the interface. (The holes are not visible to the eyes.) Then, DEHP molecules are rapidly adsorbed at the hole, which is covered by ionized DEHP. Therefore, the interfacial tension in the hole becomes much lower than that of the other CaDEHP-adsorbed interface. This triggers Marangoni instability. The instability causes macroscopic convection which removes the accumulated CaDEHP by agitation. As a result, the interface is reset. The adsorption of DEHP from the bulk starts again. For other cations, such aggregates do not form by ion-exchange: adsorption and desorption proceed continuously, and instability is not induced. We may consider that the nonlinearity in the ad/desorption rate plays a key role in the onset of instability. This is just a possible explanation for the ion-sensitive instability. We are currently performing experiments to examine this scenario: many preliminary experimental results support this consideration.

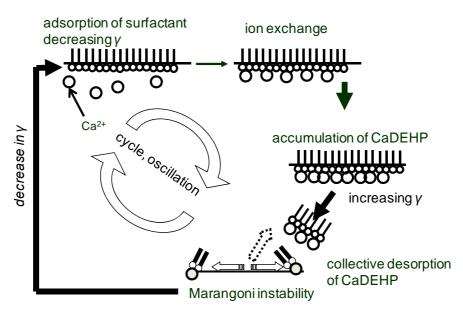
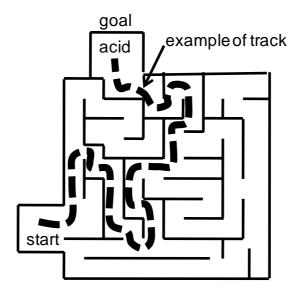


Figure 9. Cyclic change in interfacial tension.

Maze-solving droplets are another example that gives the impression of emergence. Lagzi *et al.* [41] made a maze with channels that are 1.4-mm wide and 1-mm tall and filled it with 240 μ L of KOH aqueous solution. A surfactant was added to reduce the surface tension. As shown in Figure 10, HCl solution was placed at the goal of the maze to form a pH gradient from the goal.

Figure 10. Maze-solving droplet is shown by tracing over a figure in [41].



After the gradient formed, an oil droplet containing 2-hexyldecanoic acid (HDA) was placed at the entrance of the maze. The droplet moved from the entrance to the goal on the shortest path illustrated in Figure 10. The interfacial tension between oil and water depends considerably on the pH and hence a tension gradient formed between the front and the rear of the droplet. This causes Marangoni instability, and the resulting internal convection drives the droplet. Strictly speaking, this droplet motion belongs to the category with a pretreated substrate. (The substrate in this system is the water's

surface.) However, maze-solving or path-finding problems have many applications in science and technology [42,43]. This study may inspire further study of autonomously moving objects.

Sugawara *et al.* [44,45] used the instability of an oil/water interface to realize 3D translation of droplets. Spontaneous Marangoni instability at the oil/water interface forms a pair of convection rolls that drives a droplet. A pair of convection rolls occasionally appears with Marangoni instability, which causes various kinds of regulated motions [36].

4. Autonomously Moving Vesicles

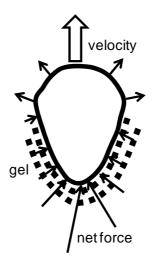
A vesicle consists of a small water-pool coated with a bilayer or multilamella membrane. It is used for various kinds of studies as a model cell, a confined reaction field, and a carrier of chemicals. Vesicles are widely studied in many fields of science. However, the study of autonomously moving vesicles is not popular, although a biological cell owes many of its functions to its motility. In contrast, amoeboid motion has been studied in biology. A sol/gel transition that is precisely controlled by many biological processes is considered to be a key factor in motility [1]. Another well-studied example of cell locomotion is the motion of *Listeria monocytogenes*, which moves by actin polymerization [46–49]. The polymerized actin network forms a gel that remains on the trail. In this case, a sol/gel transition also produces the motive force by its elastic stress. In both cases, a sol/gel transition is related to cell motility, and hence a vesicle moving with a sol/gel transition is studied. This is one of the prototypes of moving vesicles.

As mentioned in the introduction, continuous energy conversion requires a cycle, in which the physicochemical state is reset to enter the next cycle. If a vesicle undergoes oscillatory changes in shape under an appropriate chemical environment, one may regard it as a continuous energy transducer from the chemical potential into mechanical work. This type of structural change in a vesicle is also studied by several scientists. At present, this type of structural change is observed with disintegration of the vesicle [50–52]. That is, the vesicle size decreases with the repetition of the cycle. However, an attempt to construct a cyclic change in vesicle shape may be developed to design biomimetic (self-sustained) vesicle motility.

We introduce two kinds of vesicle dynamics as mentioned above. First, we introduce the earliest studies on vesicle locomotion. Transient motion is often observed; for example, the electrostatic interaction between the vesicle membrane and a substrate moves a phospholipid vesicle transiently [53]. However, self-sustained motion is achieved by mimicking the locomotion of *Listeria monocytogenes* [54,55]. The bacterium moves with a comet-like tail in cytoplasm. The protein ActA polymerizes the actin, and the gel that forms pushes the bacteria by its elastic stress. Upadhyaya *et al.* introduced ActA into the membrane of a phospholipid vesicle and immersed it in cytoplasm extract. The vesicle moves with a motion resembling that of *Listeria monocytogenes*. The propulsive force can be understood by taking into account the membrane's tension and the elastic stress of the formed gel. The net force and the vesicle's shape are illustrated in Figure 11. This understanding explains the deformation in vesicle shape and the time-course of the velocity change. Essentially the same idea is employed for an autonomously moving oil drop [56]. It contains the actin polymerization promoter VCA and moves in a cell extract. The oil drop moves by the elastic stress generated by the formed gel. The shape of the

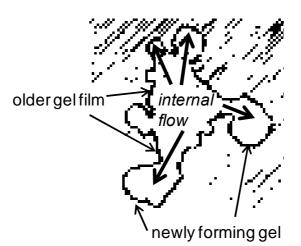
moving droplet is very similar to that of the moving vesicle, which indicates that the propulsive forces of both objects are generated by the same mechanism.

Figure 11. Shape of a vesicle that moves by actin polymerization, traced from [55]. Distribution of compression force is also traced.



For a liquid drop, another attempt has been made using a sol/gel transition. Sumino *et al.* observed the blebbing of a droplet of palmitic acid (oil) on water containing $C_{18}TAC$ [57]. Although this is droplet motion, the propulsive mechanism is that of the above-mentioned autonomously moving vesicles. Figure 12 illustrates the droplet's shape during the motion.

Figure 12. Blebbing dynamics of an oil droplet is shown by tracing a figure of [57].

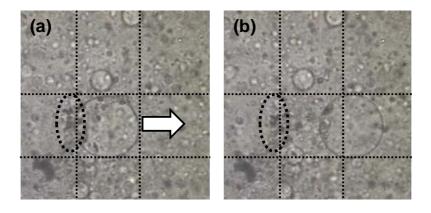


A gel-like film is formed at the oil/water interface by chemical reactions. However, the mechanical strength of the thin film is inhomogeneous, and hence part of the film ruptures because of the high internal pressure produced by the elastic stress of the film itself. Then, the internal palmitic acid emerges to create a fresh oil/water interface, at which the gel-like film forms again. Repetition of this process generates many blebs, and the resulting fluid flow of palmitic acid moves the droplet. Internal flow combined with a sol/gel transition is also a key factor in amoeboid motion. This system is

simpler, and thus the mechanism may be instructive for the design of autonomously moving objects with a sol/gel transition.

Recently, the authors' group studied an autonomously moving vesicle composed of didodecyldimethylammonium bromide (DDAB) with ion-exchange [58]. When iodide anions diffuse into the vesicular phase, ion-exchange occurs. The product didodecyldimethylammonium iodide (DDAI) is sparingly soluble in water. DDAI molecules in the vesicle membrane gather to form aggregates shown in the dotted circle of Figure 13. The formed DDAI molecules flow on the membrane towards the largest aggregate. This flow reflects the surface tension gradient of the vesicle membrane. The tension gradient is a consequence of a chemical composition gradient in the membrane. The tension gradient is accompanied by a pressure gradient in the water-pool, which induces an internal flow. This pushes the vesicle, as shown in Figure 13. Since the DDAB molecules are consumed, the vesicle size decreases monotonously. Therefore, it is an incomplete locomotion system. However, it is reasonably similar to the aforementioned vesicle locomotion since a mechanical stress generated by polymerization (aggregation) moves the vesicle.

Figure 13. Vesicle moving via ion exchange Vesicle is composed of didodecyldimethylammonium bromide at a concentration of 10 mM. Vesicle moves by diffusion of KI. The grid is drawn at the same place for both photographs. Aggregates remain after the leaving vesicle as shown in dotted circle. The right photograph is of 1.1 s after the left.



All the vesicle motions mentioned above are basically simple translations. These locomotions may be categorized as autonomously moving droplets containing $C_{18}TAC$ and iodide anions: the object moves so that the overall free energy decreases. However, the motion itself generates the local chemical composition gradient required for locomotion. For example, when considering a vesicle moving with ActA, polymerization proceeds mainly at the rear of the moving vesicle. ActA molecules are distributed over the entire membrane. Thus, the difference in polymerization rate between the front and the rear of a moving vesicle probably arises from the effect of the velocity on the polymerization rate. Such a dynamical system contains a kind of autocatalytic process, in which the velocity generated by the reaction increases the reaction rate at the front, and may be regarded as an example of self-sustained motion in this paper.

The other important topic for autonomous motion of vesicles is oscillatory changes in vesicle structure. A structural change is usually induced by the surrounding chemicals, which indicates that

the vesicle works as a continuous energy transducer from chemical potential to mechanical work. Recent studies of rhythmic pore dynamics are an example of such oscillatory changes in vesicle structure [50–52]. Typically, geometrical changes in a vesicle are considered using statistical thermodynamics. The membrane free energy is mathematically modeled, and the vesicle's shape changes so that the free energy decreases [59]. A vesicle takes the shape that yields the minimum free energy. However, this description does not include oscillatory changes in vesicle structure. Rhythmic pore dynamics, in which the repetitive opening and closing of a pore in the vesicle membrane occurs, is the simplest dynamics of oscillatory shape change. Several scientists have studied such pore dynamics [50–52], using a vesicle composed of a phospholipid bilayer. When the nonionic surfactant triton X-100 was added, a transient pore was repeatedly generated. The opening was very rapid, and the closing process was slower, resembling a relaxation process. However, after closing, the pore re-opened. The vesicle shrank during this process, and thus oscillation is imcomplete.

Kaga and Ohta mathematically explained the rhythmic pore dynamics with vesicle shrinkage as shown in Figure 14 [60,61]. According to them, the nonionic surfactant dislodges the phospholipid from the membrane, and the decreased surface area makes the membrane tense. Since the internal pressure of the vesicle rises with this higher tension, a hole opens beyond the threshold stress. Then, the internal water flows out owing to the higher internal pressure. This outflow relaxes the membrane tension, and the vesicle closes the pore. After vesicle shrinkage and closing, the same process may start again. This process is a kind of thermodynamic relaxation that dislodges lipid molecules (the vesicle constituents): once the lipid molecules are removed, the vesicle must move to another stable state. Through the transition process, the pore opens and closes. This may be regarded as a sequence of stepwise vesicle disintegration. However, the rhythmic change may provide a hint for the design of an oscillatory shape change in vesicles with a fixed size: this rhythmic dynamics occurs under the transport of lipid from the membrane to the bulk solution. In contrast, the vesicle may acquire its constituents from the surroundings so as to maintain its size, although the actual design is not easy. If this could be realized, it will resemble living matter that vesicle maintain its existence and motion by the exchange of matter and related chemical reactions.

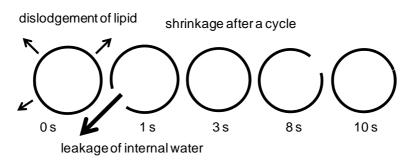


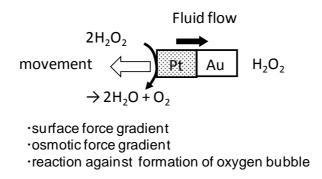
Figure 14. Schematic diagram of rhythmic pore dynamics of phospholipid vesicle.

5. Autonomously Moving Particles

Autonomously moving solid particles may develop into a new technology because many solid particles act as catalyst. If a catalytic particle moves in response to the surrounding environment to start a catalytic reaction at a predetermined reaction point, an interesting chemical system may be designed.

A concentration gradient and/or temperature gradient can move colloidal particles by diffusiophoresis and thermophoresis, respectively [62–64]. Another well-known driving force for particle motion is a surface tension gradient. This causes the Marangoni effect, resulting in tangential motion of a fluid against an adjacent solid surface. In both cases, a gradient of a thermodynamic quantity is necessary for particle motion. In an autonomously moving system, however, the gradient is spontaneously produced by an instability or autocatalytic process inherent to the system. Once the gradient forms, the particle may move by phoresis or by the Marangoni effect. (The gradient is restricted to the vicinity of the moving object.) One of the simplest systems was discovered by Paxton *et al.* [65,66] They used a rod with a length and diameter of 1 μ m and 0.37 μ m, respectively. As shown in Figure 15, about half its length is platinum and the other half is gold. When it is immersed in water containing hydrogenperoxide, it moves. The direction of motion is approximately parallel to the longer axis. The speed increases with increasing H₂O₂ concentration up to 3.3 % and then reaches a plateau.

Figure 15. Composite colloidal rod composed of platinum and gold. Platinum catalyzes the decomposition of H_2O_2 , which moves the rod.



Decomposition of H_2O_2 generates oxygen that forms bubbles in water. When we use a macroscopic object that catalyzes H_2O_2 decomposition, it can move by the mechanical reaction to bubble formation. Following Paxton *et al.*, however, the motion of the colloidal rod is not caused by bubble formation by oxygen. Although many theoretical studies have examined particle locomotion via chemical reactions [67–72], Paxton *et al.* concluded that the particles in their system moved by an interfacial energy gradient between the particle and the adjacent liquid phase [65,66].

The decomposition rate of H_2O_2 is higher on the platinum surface than on the gold surface. Therefore, a chemical composition gradient forms in solution along the longer axis of the rod. Thus, the surface energy of the rod differs between the platinum and the gold parts, generating a tangential flow because of the Marangoni effect. This is an interesting system because, in principle, the catalytic reaction moves the catalysis three dimensionally. At present, however, the motion is not fully regulated, although the rod moves approximately along the longer axis.

Nakata *et al.* successfully extracted many dynamical modes from autonomous motions of camphor and camphor floats on a water surface [73–76]. This principle of camphor motion is illustrated in Figure 16 and is undoubtedly driven by a surface tension gradient. Small piece of camphor are known to move around on the surface of water. Camphor molecules diffuse from the periphery of the piece to the water's surface. If the surface concentration of camphor is inhomogeneous along the periphery, the

surface tension depends on the position along the periphery. Then, the camphor moves towards the point with stronger surface tension (camphor free surface), as shown in Figure 16a. The induced motion is quite random.

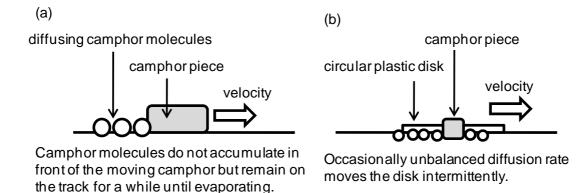


Figure 16. Principles of camphor motion for (a) a piece of camphor and (b) a camphor float.

Nakata *et al.* extracted many kinds of regulated motion. For example, they placed a piece of camphor at the center of a circular float shown in Figure 16b. A small portion of the camphor extrudes from beneath the float. The dynamical mode depends on the diameter of the float. A float with a small diameter moves continuously. Beyond a threshold diameter, the float exhibits quasi-periodic intermittent motion with an explicit mean periodicity. When the float is smaller, the driving mechanism is essentially the same as that of camphor itself on water. Though the motion is slower and appears smoother owing to the larger mass of the float, it is essentially random. As the diameter increases, it takes longer for the diffusing camphor to reach the periphery (air/water surface). The diffusion time corresponds to the induction period for the motion. After the induction period, the diffused camphor molecules reach the restricted portion of the float's periphery. The other part is free from camphor. Then, a distinct difference in surface tension forms along the float periphery, which moves the float almost abruptly. As a result, the intermittent motion is obtained, and the induction period becomes the periodicity. Owing to sublimation of camphor, the water surface is quickly refreshed.

Nakata *et al.* also succeeded in controlling the motion of a camphor boat with a surfactant-adsorbed surface. A small piece of camphor adhering to the rear of a plastic boat drives it in continuous motion. However, when surfactant molecules are adsorbed on the water's surface, the boat exhibits two dynamical modes depending on the concentration. The motion changes from continuous to intermittent modes with increasing concentration, and its further increase stops the motion. Strikingly, as the concentration increases further, the boat again moves continuously or intermittently, depending on the concentration. In general, the presence of surfactant diminishes the driving force by the Marangoni effect and tends to stop the motion, because the surfactant decreases the surface tension and its gradient. Intermittent motion appears at the border between the continuous mode and no motion. The addition of surfactant yields the intermittent motion, which is not seen in a simple camphor boat. It is interesting that the simple driving mechanism in camphor systems can produce two dynamical modes.

The autonomously moving particles treated in this paper belong to the same category as that of reactive droplets and moving vesicles because the object's motion generates a local gradient of a thermodynamic variable. Sumino *et al.* described this type of dynamics as follows [28]:

$$m\frac{d\vec{v}}{dt} = -\mu\vec{v} + \varepsilon\frac{\vec{v}}{|\vec{v}|} + \xi(t)$$
(6)

Here, *m* and *v* denote the mass and velocity of the moving object, respectively, and μ represents the viscous drag coefficient. The second term on the right-hand side expresses the system's autocatalytic nature: the velocity *v* is amplified by itself. The ε denotes a constant that expresses the strength of the autocatalytic nature. The last term is noise, which is necessary for the onset of motion. Equation 6 is phenomenological and does not contain substantial physicochemical details. For that reason, however, it may be applicable to various kinds of moving objects that undergo self-amplification of velocity. Sumino *et al.* applied Equation 6 to the motion of a reactive droplet with appropriate boundary conditions and successfully described its characteristics.

Finally, the autonomously moving objects treated in this review are categorized in Table 1. As shown in the table, the mechanism for the motion is surface energy gradient, elastic stress or diffusiophoresis. If another mechanism is found, the new idea probably comes from the studies of biological systems.

Colloidal Object	Mechanism of Motion	References
droplet	surface energy gradient	[11-45]
	elastic stress	[56,57]
vesicle	surface energy gradient	[53]
	elastic stress/membrane tension	[54,55,58]
particle	surface energy gradient	[65,66,73–76]
	diffusiophoresis, osmotic force	[62-64,67-72]

Table 1. Autonomously moving object categorized by the mechanism of motion.

6. Summary

The autonomous motion of colloidal objects was reviewed, focusing on droplets, vesicles and solid particles. After an introductory discussion of the relationship between emergence and nonlinear dynamics, droplet motion was studied, primarily droplet motion driven by chemical reactions. Droplet exhibits various kinds of motion such as translation, oscillatory shape change, kicking, and rotation. They are driven by wetting transitions and Marangoni instability. The dynamical modes can be controlled by managing the surrounding chemical conditions. Autonomous vesicle motion was reviewed focusing on the study of sol/gel processes. This type of study is inspired by biological systems such as amoeboid motion and that of *Listeria monocytogenes*. When a protein that polymerizes actin is embedded in the vesicle, it moves in manner similar to *Listeria monocytogenes*. The same mechanism is used for droplet motion. Much simpler motion with sol/gel dynamics is achieved for an oil droplet on the water surface of water. An inhomogeneous gelation at the interface triggers an internal flow that drives the droplet. Furthermore, simple ion exchange in a DDAB vesicle also moves the vesicle. In the last section, we discussed the locomotion of catalytic particles, which is

caused by phoresis and/or Marangoni effect. A gradient of a thermodynamic variable which is necessary for the effect is generated by the particle's structure. We also discussed the motion of camphor on the surface of water. The camphor is driven by surface tension, and the gradient required for motion is generated by the velocity itself. Some mathematical treatments of the autonomous motions were introduced and discussed with the corresponding experimental results. Autonomously moving colloidal objects obtain the required energy from surface reactions and can respond to changes in the surrounding chemical conditions. Thus, they resemble living matter. Because of these characteristics, these moving systems attract much scientific interest and have the potential to affect future technologies.

References

- Lodish, H.; Berk, A.; Matsudaira, P.; Kaiser, C.A.; Krieger, M.; Scott, M.P.; Zipursky, S.L.; Darnell, J. *Molecular Cell Biology*, 5th ed.; W. H. Freeman and Company: New York, NY, USA, 2004.
- 2. Sterling, C.V.; Scriven, L.E. Interfacial turbulence: Hydrodynamic instability and the marangoni effect. *AIChE* **1959**, *5*, 514–523.
- 3. Pearson, J.R.A. On convection cells induced by surface tension. J. Fluid Mech. 1958, 4, 489–500.
- 4. Brian, P.L.T.; Smith, K.A. Influence of Gibbs adsorption on oscillatory Marangoni instability. *AIChE* **1972**, *18*, 231–233.
- 5. Hilborn, R.C. *Chaos and Nonlinear Dynamics an Introduction for Scientists and Engineers*, 2nd ed.; Oxford University Press Inc.: New York, NY, USA, 2000.
- 6. Colinet, P.; Legros, J.C.; Verlarde, M.G. Nonlinear Dynamics of Surface-Tension-Driven Instabilities; Wiley-VCH Verlag: Berlin, Germany, 2001.
- 7. Bird, R.B.; Stewart, W.E.; Lightfoot, E.N. *Transport Phenomena*; John Wiley & Sons, Inc.: New York, NY, USA, 1960.
- 8. Zhabotinskii, A.M. Periodic course of oxidation of malonic acid in solution (investigation of the kinetics of the reaction of Belousov). *Biophysics* **1964**, *9*, 329–335
- 9. Field, R.J.; Noyes, R.M. Oscillations in chemical systems. IV. Limit cycle behavior in a model of a real chemical reaction. *J. Chem. Phys.* **1974**, *60*, 1877–1884.
- Tyson, J.J.; Fife, P.C. Target patterns in a realistic model of the Belouzov-Zhabotinskii reaction. J. Chem. Phys. 1980, 73, 2224–2237.
- 11. Chaudhury, M.K.; Whitesides, G.M. How to make water run uphill. Science 1992, 256, 1539–1541.
- 12. Santos, F.D.D.; Ondarcuhu, T. Free-running droplets. Phys. Rev. Lett. 1995, 75, 2972-2975.
- 13. Lee, S.W.; Laibinis, P.E. Directed movement of liquids on patterned surfaces using noncovalent molecular adsorption. J. Am. Chem. Soc. 2000, 122, 5395–5396.
- 14. Ichimura, K.; Oh, S.K.; Makagawa, M. Light-driven motion of liquids on a photoresponsive surface. *Science* **2000**, 288, 1624–1626.
- 15. Wasan, D.T.; Nikolov, A.D.; Brenner, H. Droplets speeding on surfaces. Science 2001, 291, 605–606.
- 16. Daniel, S.; Chaudhury, M.K.; Chen, J.C. Fast drop movements resulting from the phase change on a gradient surface. *Science* **2001**, *291*, 633–636.
- 17. Bain, C.D. Motion of liquids on surfaces. ChemPhysChem 2001, 2, 580-582.
- 18. de Gennes, P.G. The dynamics of reactive wetting on solid surfaces. *Physica A* 1998, 249, 196–205.

- 19. Nakache, E; Dupeyrat, M.; Vignes-Adler, M. The contribution of chemistry to new Marangoni mass-transfer instabilities at the oil/water interface. *Faraday Discuss. Chem. Soc.* **1984**, 77, 189–196.
- 20. Nakache, E.; Dupeyrat, M. Chemical reactions and oscillating potential difference variations at an oil-water interface. *Bioelectrochemistry* **1982**, *9*, 583–590.
- 21. Kai, S.; Muller, S.C.; Mori, T.; Miki, M. Chemically driven nonlinear waves and oscillations at an oil-water interface. *Physica D* **1991**, *50*, 412–428.
- 22. Yoshikawa, K.; Magome, M. Chemomechanical Transduction in an oil-water system. Regulation of the macroscopic mechanical motion. *Bull. Chem. Soc. Jpn.* **1993**, *66*, 3352–3357.
- 23. Miura, T. Department of Chemical Engineering & Materials Science, Doshisha University, Kyotanabe, Kyoto, Japan. Private Communications in Doshisha University, 2009.
- 24. Shioi, A.; Katano, K.; Onodera, Y. Effect of solid walls on spontaneous wave formation at water/oil interfaces. *J. Coll. Int. Sci.* 2003, 266, 415–421.
- 25. Atkin, R.: Craig, V.S.J.; Wanless, E.J.; Biggs, S. Mechanism of cationic surfactant adsorption at the solid-aqueous interface. *Adv. Colloid Interface Sci.* **2003**, *103*, 219–304.
- 26. Kuragane, S.; Fujii, T.; Ban, T.; Shioi, A. Spontaneous wave driven by chemical autophobing with oscillatory dynamics at glass/oil/water interfaces *Colloid. Surface. A* **2007**, *311*, 16–25.
- 27. Kitahata, K.; Yoshikawa, K. Chemo-mechanical energy transduction through interfacial instability. *Physica D* **2005**, *205*, 283–291.
- Sumino, Y.; Magome, N.; Hamada, T.; Yoshikawa, K. Self-running droplet: Emergence of regular motion from nonequilibrium noise. *Phys. Rev. Lett.* 2005, *94*, 068301.
- 29. Sumino, Y.; Kitahata, H.; Yoshikawa, K.; Nagayama, M.; Nomura, S.M.; Magome, N; Mori, Y. Chemosensitive running droplet. *Phys. Rev. E* **2005**, *1672*, 041603.
- 30. Ban, T.; Suzuki, S.; Abe, S.; Shioi, A. Anionic control of autonomous motion of oil/water interface with cationic surfactant. *Chem. Lett.* **2007**, *36*, 1040–1041.
- Ban, T.; Shioi, A. Autonomous motion of liquids interface controlled by chemical reaction. In *Chemical Reaction on Surfaces*; Duncan, J.I., Klein, A.B., Eds.; Nova Science Publishers, Inc.: Hauppauge, NY, USA, 2008; pp.155–194.
- 32. Shioi, A.; Ban, T.; Suzuki, S. Noise-induced kinetic model for autonomous motion of contact line in oil/water system with chemical reaction. *Phy. Rev. E* **2008**, *77*, 036208.
- Morimune, Y.; Sugiyama, T.; Ban, T.; Shioi, A. Traveling wave patterns reproduced by a simple model for oil/water interface–Transducer of chemical potential into work–. *Int. J. Soc. Mat. Eng. Resources* 2010, 17, 115–119.
- 34. Shioi, A.; Ban, T.; Suzuki, S. Model of traveling wave formed by noise-induced autonomous motion of contact line with oil/water interface. *Chem. Phys. Lett.* **2008**, *467*, 210–215.
- 35. Lewis, J.B.; Pratt, H.R.C. Oscillating droplets. Nature 1953, 171, 1155–1156.
- 36. Ban, T.; Hatada, Y.; Takahashi, K. Spontaneous motion of a droplet evolved by resonant oscillation of a vortex pair. *Phys. Rev. E* **2009**, *79*, 031602.
- 37. Shioi, A.; Sugiura, Y.; Nagaoka, R. Oscillation of interfacial tension at liquid/liquid interface composed of di(2-ethylhexyl) phosphoric acid and calcium chloride. *Langmuir* **2001**, *17*, 4189–4195.
- Shioi, A.; Kumagai, H.; Sugiua, S.; Kitayama, Y. Oscillation of interfacial tension and spontaneous interfacial flow at water/oil interface composed of di(2-ethylhexyl) phosphoric acid. *Langmuir* 2002, 18, 5516–5522.

- Shioi, A.; Yamada, K.; Shiota, R.; Hase, F.; Ban, T. Chemically driven tension fluctuation and motion of interface with divalent cation and di(2-ethylhexyl)phosphoric acid. *Bull. Chem. Soc. Jpn.* 2006, 79, 1696–1703.
- 40. Ban, T.; Kurisaka, K.; Fujii, T.; Shioi, A. Ionic control of droplet motion. *Chem. Lett.* **2006**, *35*, 1134–1135.
- 41. Lagzi, I.; Soh, S.; Wesson, P.J.; Browne, K.P.; Grzybowski, B.A. Maze solving by chemotactic droplets. J. Am. Chem. Soc. 2010, 132, 1198–1199.
- 42. Nakagaki, T.; Yamada, H.; Toth, A. Path finding by tube morphogenesis in an amoeboid organism. *Biophys. Chem.* **2001**, *92*, 47–52.
- 43. Tero, A; Kobayashia, R.; Nakagaki, T. Physarum solver: A biologically inspired method of road-network navigation. *Physica A* **2006**, *363*, 115–119.
- 44. Toyota, T.; Maru, N.; Hanczyc, M.M.; Ikegami, T.; Sugawara, T. Self-propelled oil droplets consuming "fuel" surfactant. J. Am. Chem. Soc. 2009, 131, 5012–5013.
- 45. Hanczyc, M.M.; Toyota, T.; Ikegami, T.; Packard, N.; Sugawara, T. Fatty acid chemistry at the oil-water interface: Self-propelled oil droplets. *J. Am. Chem. Soc.* **2007**, *129*, 9386–9391.
- 46. Peskin, C.S.; Odell, G.M.; Oster, G.F. Cellular motions and thermal fluctuations: The Brownian ratchet. *Biophys. J.* **1993**, *65*, 316–324.
- 47. Mogilner, A.; Oster, G. Cell motility driven by actin polymerization. *Biophys. J.* 1996, 71, 3030–3045.
- 48. Gerbal, F.; Chaikin, P.; Rabin, Y.; Prost, J. An elastic analysis of Listeria monocytogenes propulsion. *Biophys. J.* **2000**, *79*, 2259–2275.
- 49. Mogilner, A.; Oster, G. Force generation by actin polymerization II: The elastic ratchet and tethered filaments. *Biophys. J.* **2003**, *84*, 1591–1605.
- 50. Nomura, F.; Nagata, M.; Inaba, T.; Hiramatsu, H.; Hotani, H.; Takiguchi, K. Capabilities of liposomes for topological transformation. *Proc. Nat. Acad. Sci.* **2001**, *98*, 2340–2345.
- 51. Umeda, T.; Nomura, F.; Inaba, T.; Takiguchi, K.; Hotani, H. Stepwise shrinkage of liposomes driven by thermal fluctuations of the membranes. *ChemPhysChem* **2005**, *6*, 1047–1050.
- 52. Hamada, T.; Hirabayashi, Y.; Ohta, T.; Takagi, M. Rhythmic pore dynamics in a shrinking lipid vesicle. *Phys. Rev. E* **2009**, *80*, 051921.
- 53. Solon, J.; Streicher, P.; Richter, R.; Brochard-Wyart, F.; Bassereau, P. Vesicles surfing on a lipid bilayer: Self-induced haptotactic motion. *Proc. Nat. Acad. Sci.* **2006**, *103*, 12382–12387.
- 54. Giardini, P.A.; Fletcher, D.A.; Theriot, J.A. Compression forces generated by actin comet tails on lipid vesicles. *Proc. Nat. Acad. Sci.* **2003**, *100*, 6493–6498.
- Upadhyaya, A.; Chabot, J.R.; Andreeva, A.; Samadani, A.; Oudenaarden, A. Probing polymerization forces by using actin-propelled lipid vesicles. *Proc. Nat. Acad. Sci.* 2003, 100, 4521–4526.
- 56. Boukellal, H.; Campás, O.; Joanny, J.-F.; Prost, J.; Sykes, C. Soft Listeria: Actin-based propulsion of liquid drops. *Phys. Rev. E* **2004**, *69*, 061906.
 - 57. Sumino, Y.; Kitahata, H.; Seto, H.; Yoshikawa, K. Blebbing dynamics in an oil-water-surfactant system through the generation and destruction of a gel-like structure. *Phys. Rev. E* **2007**, *76*, 055202.
- 58. Miura, T.; Oosawa, H.; Sakai, M.; Syundo, Y.; Ban, T.; Shioi, A. Autonomous motion of vesicles via ion exchange. *Langmuir* **2010**, *26*, 1610–1618.

- 59. Seifert, U. Configurations of fluid membranes and vesicles. Adv. Phys. 1997, 46, 13–137.
- 60. Kaga, M.; Ohta, T. Shrinkage dynamics of a vesicle in surfactant solutions. *Eur. Phys. J. E* 2006, 21, 91–98.
- 61. Kaga, M.; Ohta, T. Shrinkage dynamics of a vesicle induced by chemical reactions. J. Phys. Soc. Jpn. 2007, 76, 094003.
- 62. Anderson, J.L. Colloid transport by interfacial forces. Ann. Rev. Fluid Mech. 1989, 21, 61-99.
- 63. Anderson, J.L.; Lowell, M.E.; Prive, D.C. Motion of a particle generated by chemical gradient Part 1. Non-electrolytes. *J. Fluid Mech.* **1982**, *117*, 107–121.
- 64. Prieve, D.C.; Anderson, J.L.; Ebel, J.P.; Lowell, M.E. Motion of a particle generated by chemical gradient. Part 2. Electrolytes. *J. Fluid Mech.* **1984**, *148*, 247–269.
- Paxton, W.F.; Kevin, K.C.; Kistler, C.; Christine, C.Olmeda, C.; Sen, A.; Angelo, S.K.; Cao, Y.; Mallouk, T.E.; Lammert, P.E.; Crespi, V.H. Catalytic nanomotors: Autonomous movement of striped nanorods. J. Am. Chem. Soc. 2004, 126, 13424–13431.
- 66. Paxton, W.F.; Baker, P.T.; Kline, T.R.; Wang, Y.; Mallouk, T.E.; Sen, A. Catalytically induced electrokinetics for motors and micropumps. J. Am. Chem. Soc. 2006, 128, 14881–14888.
- 67. Golestanian, R.; Liverpool, T.B.; Ajdari, A. Propulsion of a molecular machine by asymmetric distribution of reaction products. *Phys. Rev. Lett.* **2005**, *94*, 220801.
- 68. Kung, H.H.; Kung, M.C. Catalytic nanomotors-promising leads for new catalytic applications. *Appl. Catal. A Gen.* **2006**, *309*, 159–161.
- 69. Tao, Y.G.; Kapral, R. Design of chemically propelled nanodimer motors. J. Chem. Phys. 2008, 128, 164518.
- Cordova-Figueroa, U.M.; Brady, J.F. Osmotic propulsion: The osmotic motor. *Phys. Rev. Lett.* 2008, 100, 158303.
- 71. Tao, Y.G.; Kapral, R. Dynamics of chemically powered nanodimer motors subject to an external force. *J. Chem. Phys.* **2009**, *131*, 024113.
- 72. Bertin, E.; Droz, M.; Gregoire, G. Hydrodynamic equations for self-propelled particles: Microscopic derivation and stability analysis. *J. Phys. A Math. Theor.* **2009**, *42*, 445001.
- 73. Nakata, S.; Doi, Y.; Kitahata, H. Synchronized sailing of two camphor boats in polygonal chambers. *J. Phys. Chem. B* **2005**, *109*, 1798–1802.
- Nakata, S.; Kawagishi, N.; Murakami, M.; Suematsu, N.J.; Nakamura, M. Intermittent motion of a camphor float depending on the nature of the float surface on water. *Colloid. Surface. A* 2009, 349, 74–77.
- Suematsu, N.J.; Ikura, Y.; Nagayama, M.; Kitahata, H.; Kawagishi, N.; Murakami, M.; Nakata, S. Mode-switching of the self-motion of a camphor boat depending on the diffusion distance of camphor molecules. J. Phys. Chem. C 2010, 114, 9876–9882.
- 76. Nakata, S.; Murakami, M. Self-motion of a camphor disk on an aqueous phase depending on the alkyl chain length of sulfate surfactants. *Langmuir* **2010**, *26*, 2414–2417.

© 2010 by the authors; licensee MDPI, Basel, Switzerland. This article is an open access article distributed under the terms and conditions of the Creative Commons Attribution license (http://creativecommons.org/licenses/by/3.0/).